0026-895X/95/020272-11$03.00/0

MOLECULAR PHARMACOLOGY, 47:272-282, 1995.

Differential *In Vivo* Induction of Immediate Early Genes by Oxotremorine in the Central Nervous System of Long- and Short-Sleep Mice

LEONIDAS TSIOKAS[1] and MARK WATSON

Department of Pharmacology and Toxicology, University of Medicine and Dentistry of New Jersey, New Jersey Medical School and the Graduate School of Biomedical Sciences, Newark, New Jersey 07103-2714

Received March 1, 1994; Accepted October 19, 1994

SUMMARY

Long-sleep (LS) and short-sleep (SS) mice show differential sensitivity to both acute and chronic ethanol administration. Previous data also showed differential behavioral responses to muscarinic acetylcholine receptor agonist or antagonist treatment. We now report significantly greater inductions of c-*fos*, c-*jun*, *jun*-B, and *Egr*-1, but not *jun*-D, mRNA in the central nervous system (CNS) of LS versus SS mice after the intraperitoneal administration of oxotremorine. These genomic responses were dose dependent and completely inhibited (in both strains) by scopolamine, a specific muscarinic receptor antagonist. *In situ* hybridization studies verified the greater immediate early gene (IEG) inductions in LS mice, as initially observed by Northern analysis, and specifically showed that c-*fos* mRNA induction occurred predominantly in the thalamus, olfactory bulb, cerebellum, and cerebral cortex. Oxotremorine-induced c-*jun* mRNA was increased in cerebellum, CA1 hippocampal field, and cerebral cortex of both strains. Induced *jun*-B and *Egr*-1 transcripts were determined to have very similar CNS distribution patterns. Both mRNA species were induced in the cerebral cortex, caudate nucleus and putamen, hippocampal structures, and olfactory bulb. To further determine whether these differential IEG inductions reflect regional differences in receptor numbers, we determined the distributions and levels of each of the five muscarinic receptor subtypes in both strains by *in situ* hybridization. These data show that differences in receptor numbers alone may not account for the differential IEG inductions observed between the strains. Differential coupling constraints among CNS muscarinic receptors in LS versus SS mouse CNS may also play a significant role in producing differential IEG inductions.

Ethanol is a widely consumed drug and it is responsible for more preventable morbidity and mortality than all other drugs combined, with the exception of tobacco. Ethanol intoxication seriously impairs CNS function, which may result in memory impairment, psychoses, brain damage, sensory and motor disturbances, reduction in rapid eye movement sleep, and eventually anesthesia. Interestingly, similar pharmacodynamic profiles may be seen after chronic treatment with centrally acting mAChR antagonists such as scopolamine or atropine. Central acetylcholine levels are significantly affected by ethanol (1). Ethanol inhibits acetylcholine release in cortical and subcortical regions of the rodent CNS (2–4) and results in a decreased acetylcholine content in these areas and a subsequently increased density of the mAChR subtypes in these areas (5–7), presumably via a compensatory up-regulatory mechanism.

Consistent with the idea that ethanol affects cholinergic function, LS and SS mice, which were selectively bred to fix genes responsible for high and low ethanol sensitivity, respectively (8), were found to differentially respond to mAChR agonist and antagonist treatment (9, 10). Moreover, centrally administered cholinergic agonists such as carbachol, a potent cholinergic agonist, or oxotremorine, a less efficacious agonist, were able to enhance ethanol-induced sleep times in SS but not LS mice (11). In these studies, cholinergic antagonists such as atropine or pirenzipine did not have an effect on ethanol-induced sleep time in either strain when administered alone, but they were able to effectively inhibit mAChR agonist-enhanced ethanol sensitivity in SS mice. These data suggest that LS and SS mice may differ genetically in neuronal processes activated by specific mAChR agonists (11).

To correlate this differential responsiveness at the behavioral

This work was supported by National Institutes of Mental Health Grant MH43024 (M.W.) and an Advanced Predoctoral Fellowship in Pharmacology/Toxicology sponsored by the Pharmaceutical Manufacturers Association Foundation (L.T.) A preliminary presentation of these data was made at the XIth International Congress of Pharmacology (IUPHAR) in Amsterdam, The Netherlands (July 1990), and at the Fifth International Symposium on Muscarinic Receptor Subtypes in Newport Beach, CA (October 1992).

[1] Present address: Department of Medicine, Renal Division DA 517, Beth Israel Hospital, Harvard Medical School, 330 Brookline Ave., Boston, MA 02215.

ABBREVIATIONS: CNS, central nervous system; mAChR, muscarinic acetylcholine receptor; LS, long sleep; SS, short sleep; IEG, immediate early gene; kb, kilobase(s); bp, base pair(s); SSPE, saline/sodium phosphate/EDTA; SDS, sodium dodecyl sulfate; PBS, phosphate-buffered saline; SSC, saline/sodium citrate; PTX, pertussis toxin.

level with a biochemical change, we investigated mAChR-induced genomic responses in terms of the induced expression of several IEGs in discrete areas in the CNS of LS and SS mice. The present data show for the first time that mAChR activation may result in the coordinated and region-specific induction of several IEGs in the murine CNS. Furthermore, the expression of c-*fos*, c-*jun*, *jun*-B, and *Egr*-1 is differentially regulated in the CNS of LS and SS mice in response to oxotremorine. Genetic differences in the signaling pathways triggered by mAChR activation that result in the induction of c-*fos*, c-*jun*, *jun*-B, and *Egr*-1 may be responsible for differential molecular mechanisms underlying ethanol sensitivity in mice.

Materials and Methods

Animals. LS and SS mice were initially obtained from the Insitute for Behavioral Genetics at Boulder (Boulder, CO). Two separate colonies of LS and SS mice were developed by brother-sister inbreeding. Six to 10 adult male LS or SS mice of the same age (80–90 days) from each generation were tested in parallel for ethanol sensitivity. All comparisons of the duration of the loss of the righting reflex produced by a single intraperitoneal ethanol injection (4 or 5 g/kg ethanol for LS or SS mice, respectively) verified that the phenotypic trait was successfully maintained throughout the inbreeding process. Adult male mice (80–90 days) from LS and SS strains were treated with oxotremorine (4 mg/kg) and sacrificed at the following time points: 0, 15, 30, 45, 60, 90, 120, and 180 min after drug treatment. In dose-response studies, mice were treated with oxotremorine (0–5 mg/kg) and sacrificed 60 min after the drug treatment. During the scopolamine treatment, LS and SS mice were treated with either saline, oxotremorine (4 mg/kg), scopolamine (10 mg/kg), or scopolamine (10 mg/kg) 15 min before oxotremorine (4 mg/kg) and were then sacrificed 60 min after the final treatment. For *in situ* hybridization studies, LS and SS mice were given injections of 4 mg/kg oxotremorine or physiological saline solution and sacrificed 60 min after drug administration. All drugs were given as single intraperitoneal injections.

Drugs and reagents. [^{32}P]CTP (800 Ci/mmol), ^{35}S-dATP (3000 Ci/mmol), and [^{33}P]UTP (2,000 Ci/mmol) were purchased from New England Nuclear (Boston, MA). Oxotremorine susquifumarate was purchased from Aldrich Chemicals and scopolamine was purchased from Sigma Chemical Co. (St. Louis, MO). The *in vitro* transcription and subcloning kits were purchased from Promega (Madison, WI).

Probes. Plasmids carrying full length rat c-*fos* and c-*jun* cDNAs (2.2 and 1.8 kb, respectively) were gifts from T. Curran (Roche) (12), a 300-bp *Bgl*II/*Rsa*I non-zinc finger region of the mouse *Egr*-1 cDNA from V. P. Sukhatme (Harvard) (13), full length mouse *jun*-B and *jun*-D inserts (1.5 and 1.4 kb) from R. Bravo (Bristol Myers-Squibb) (14), and a 600-bp chicken β-actin cDNA from I. Creese (Rutgers). To generate specific probes appropriate for *in situ* hybridization, a 440-bp (*Eco*RI/*Sal*I) fragment of the c-*fos* cDNA, a 390-bp (*Bam*HI/*Bam*HI) fragment of the *jun*-B cDNA, or a 600-bp (*Acc*I/*Acc*I) fragment of the *jun*-D cDNA was subcloned into the pGEM-3z plasmid vector. A 650-bp fragment of the c-*jun* cDNA was made by deleting an *Acc*I/*Acc*I fragment encompassing positions 650–1800 of the full length cDNA, which was originally subcloned into the pGEM-4 vector (12). All of the resulting fragments contained mainly sequences of the 5′ untranslated regions and portions of the coding regions. Plasmids bearing full length or truncated cDNAs were linearized with appropriate restriction enzymes and were subsequently used to generate ^{32}P-labeled antisense riboprobes for Northern RNA analyses, whereas only linearized plasmids carrying specific fragments of the cDNAs were used to generate ^{33}P-labeled sense and antisense riboprobes for *in situ* hybridization. The *in vitro* transcription reactions were done according to the manufacturer's directions (Promega). Briefly, 1 μg of linearized plasmid was transcribed by 15–20 units of the appropriate RNA polymerase in a reaction mixture containing 40 mM Tris·HCl, pH 7.9, 6 mM $MgCl_2$, 2 mM spermidine, 10 mM NaCl, 0.01 M dithiothreitol, 1 unit of RNasin ribonuclease inhibitor, 500 μM ATP, 500 μM GTP, 500 μM UTP, 12 μM CTP, and 3.125 μM [^{32}P]CTP (800 Ci/mmol, 50 μCi at 10 mCi/ml). To synthesize [^{33}P]UTP-labeled riboprobes, the concentrations of unlabeled UTP and [^{33}P]UTP were adjusted to 6 μM and 1.25 μM, respectively. The total volume of all *in vitro* transcription reactions was 20 μl. The mixture was incubated for 60 min at 37–40°. After *in vitro* transcription reactions, plasmid DNA was digested with RQ1 RNase-free DNase and synthetic RNA was extracted once with phenol/chloroform saturated with 10 mM Tris·HCl, 0.1 mM EDTA, pH 8.0, and once with chloroform/isoamyl alcohol (49:1) and was precipitated in the presense of 2.5 M ammonium acetate and 75% ethanol at −70° for at least 30 min. The pellet was washed with 70% ethanol, air dried, and dissolved in 50 μl of diethylpyrocarbonate-treated water. ^{32}P- or ^{33}P-labeled riboprobes had specific activities of 0.33×10^9 or 0.9×10^9 cpm/μg, respectively. ^{33}P-labeled riboprobes used for *in situ* hybridization were partially hydrolyzed to an average mass of 100 bp, according to the method of Cox *et al.* (15), before hybridization.

A synthetic oligonucleotide probe complementary to the base 4–51 sequence of the rat m1 mRNA was purchased from Custom Oligos and labeled at the 3′ end, using terminal transferase and [^{35}S]dATP, to specific activity of 0.3×10^9 dpm/μg. Similar parallel studies were also performed for m2–m5 mAChR mRNAs.

RNA isolation and Northern blotting. Brain tissues were homogenized and total RNA was prepared by the guanidine isothiocyanate method (16). Acceptable RNA samples had A_{260}/A_{280} ratios of 1.8–2.0. Ten micrograms of RNA of each sample were fractionated by electrophoresis on 1.2% agarose/6.6% (w/v) formaldehyde gels, transferred to nylon membranes (Nytran; Schleicher & Schuell) by capillary blotting, and immobilized by both cross-linking and baking at 80° for 2 hr. Positions of the 18 S and 28 S rRNAs, as well as RNA integrity and equal loading in each lane, were examined by ethidium bromide staining of the RNA on the membranes. Membranes were prehybridized for 4 hr at 60° in a mixture containing 50% deionized formamide, 5× SSPE (1× SSPE is 0.15 M NaCl, 0.01 M NaH_2PO_4, 0.001 M EDTA, pH 7.4), 1% SDS, and 0.1 mg/ml single-stranded salmon sperm DNA. The membranes were then hybridized overnight with 1×10^6 cpm/ml ^{32}P-labeled antisense riboprobe under the same conditions as used for the prehybridization. After hybridizations, membranes were washed three times with 1× SSPE/0.5% SDS at 65° for 15 min each time and then once with 0.1× SSPE/0.5% SDS at 60° for 15 min. Membranes were exposed to Hyperfilm-MP film (Amersham) for 1–3 days at −70°, with an intensifying screen. Relative abundances of specific mRNAs were determined with a Hoefer Scientific or Shimadzu scanning densitometer.

***In situ* hybridization histochemistry.** The protocol was adapted from the method of Baldino *et al.* (17), with slight modifications. Whole mouse brains were rapidly excised, quick-frozen over dry ice, and stored at −70°. Immediately before use, mouse brains were removed from storage at −70° and fixed onto cryostat solid supporters. Serial sagittal sections (7 μm) were made with the use of a Hacker or Damon cryostat maintained at −14° and were thaw-mounted onto gelatin/chromium potassium sulfate-subbed slides. Sections were fixed for 5 min in 3% paraformaldehyde in 0.1 M phosphate-buffered saline (PBS) containing 0.02% diethylpyrocarbonate and were quickly rinsed twice in 0.1 M PBS/2× saline/sodium citrate (SSC) (1× SSC is 0.15 M NaCl, 0.015 M sodium citrate, pH 7.0) for 1 min each time. Acetylation of negative charges was performed by rinsing the slides in 0.1 M triethanolamine, pH 8.0, containing 125 μl of acetic anhydride/50 ml of the solution. Sections were then rinsed in 0.1 M PBS/2× SSC for 1 min. A 30-min rinse in 0.1 M Tris/glycine, pH 7.0, was followed by two 1-min rinses in 2× SSC, and then sections were dehydrated with increasing concentrations of ethanol in water and air dried on racks. Each section was incubated with 30 μl of hybridization mixture containing 40% deionized formamide, 10% dextran sulfate, 1× Denhardt's solution, 4× SSC, 10 mM dithiothreitol, 1 mg/ml yeast tRNA, 1 mg/ml single-stranded salmon sperm DNA, and 1.5×10^5 cpm (or 0.25 ng/section) of partially

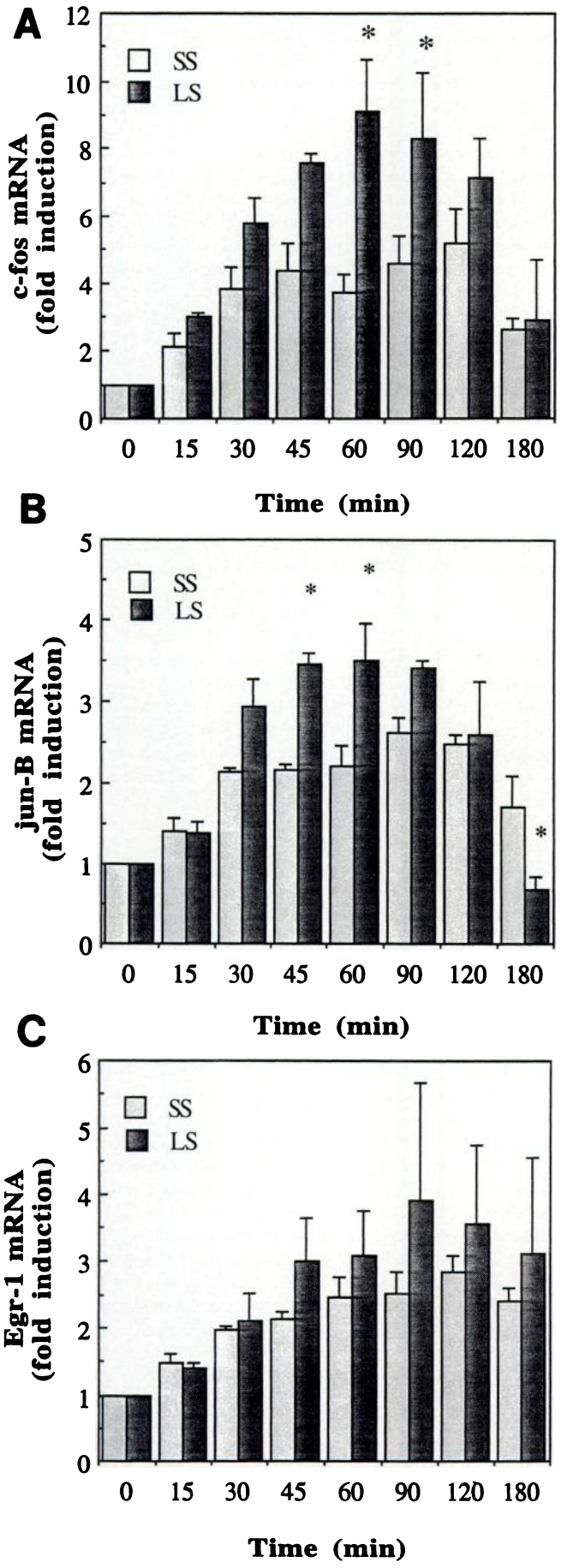

hydrolyzed ^{33}P-labeled probe. Negative control sections were incubated with probes of the sense orientation under the same conditions as described for the experimental sections. Hybridizations were carried out at 50° overnight, in a humidified chamber to prevent drying of the sections. On the following day, slides were washed twice in 50% deionized formamide/2× SSC at 52°, for 5 and 20 min, and then nonspecific background labeling was removed by incubation at 37° for 30 min in 2× SSC containing 100 μg/ml RNase A. Two quick dips in 2× SSC were followed by a 5-min rinse with 50% deionized formamide/2× SSC at 52°. Sections were then cleared with 2× SSC/0.05% Triton X-100 by gentle agitation at room temperature overnight. On the next day, sections were dehydrated in a gradually increasing series of ethanol in 300 mM ammonium acetate and were demyelinated with two rinses in xylenes, for 5 and 30 min. Finally, the sections were rinsed twice with 100% ethanol for 5 min, air dried, and exposed to Hyperfilm β-max for 4 weeks at −70°. *In situ* hybridization histochemistry using m1–m5 oligomers was performed as described previously (18–20).

Autoradiographic image analysis. The relative levels of mRNA in each specific CNS region were quantified using densitometric techniques with an IBM AT/PC-based image analysis system (DUMAS; Drexel University, Philadelphia, PA) equipped with a MV9015-H monochrome microvideo camera (Circon). Relative density values were expressed in nanocuries/microgram of grey matter tissue by reference to ^{14}C-microscale standards (Amersham) (21). A linear regression curve for the standards was generated and used to obtain relative density values corresponding to various experimental grey matter regions. Negative control sections for riboprobes received sense probes. Also, a 100-fold excess of unlabeled m1 or other oligonucleotide probe was used to obtain values corresponding to background densities in various brain areas.

Assay of mAChR-induced inositol phosphate hydrolysis. The responsiveness of genotypes to mAChR agonist-induced inositol phosphate hydrolysis was examined. Potency for mediating hydrolysis in LS and SS mouse cerebral cortex was determined using our previously described techniques. Slices (350 × 350 μm) were prepared using a McIllwain tissue chopper. Prelabeling of slices was done with [^{3}H] inositol (0.5 μM), and subsequent washing was done for 1 hr in aerated Krebs-Ringer bicarbonate buffer with 10 mM LiCl. The mAChR-stimulated breakdown was initiated by addition of 930 μl of chloroform/methanol (1:2). After 15 min at 25°, 310 μl of chloroform and 310 μl of water were added. Samples were vortex-mixed and centrifuged (4200 × *g*) for 15 min, and 750 μl of aqueous upper layer were removed for analysis of [^{3}H]inositol-1-phosphate with a formate ion exchange resin (Bio-Rad). Resins were washed four times with 5.0 mM unlabeled *myo*-inositol. Labeled inositol-1-phosphate was eluted with 0.2 M ammonium formate/0.1 M formic acid and counted by liquid scintillation.

Results

Induction Kinetics of IEG Expression

c-*fos*. The intraperitoneal injection of 4 mg/kg oxotremorine was found to produce a significant increase in the levels of brain c-*fos* mRNA (Fig. 1A). The c-*fos* mRNA induction profiles were different between SS and LS mice. The maximum c-*fos* mRNA accumulation was achieved at the 60-min time point and was 9-fold higher than basal levels in LS mice. At the same time point, oxotremorine produced a 3.7-fold induction of c-*fos* mRNA in SS mice, which was significantly lower than the

Fig. 1. Summary of the results obtained by Northern analysis, showing the time course of induction of c-*fos* (A), *jun*-B (B), and *Egr*-1 (C) mRNA in the CNS of SS and LS mice. mRNA increases induced by oxotremorine are expressed as fold induction over basal levels at the indicated time points and represent the means ± standard errors of three independent experiments. Minor differences in RNA loading were normalized by β-actin hybridization. *, Significant differences between hybridization signals, determined by Duncan's multiple range test, $p < 0.05$.

response observed in LS mice (Fig. 1A). Significant differences in the magnitude of the fold induction over basal levels for c-*fos* mRNA were also seen at the 90-min time point, where oxotremorine produced a 4.5-fold induction in SS mice, in contrast to an 8.3-fold induction in the LS mice (Fig. 1A). Both strains were found to express extremely low basal levels of c-*fos* mRNA. To obtain an accurate determination of basal levels, SS and LS basal levels were directly compared or expressed as percentages of the maximum responses, which were arbitrarily set at 100%. Both determinations showed that SS c-*fos* mRNA basal levels were 2-fold higher than LS basal levels ($p < 0.05$).

c-*jun*. Oxotremorine produced a significant accumulation of two c-*jun* mRNA species, with estimated sizes of 2.9 and 3.2 kb, in both SS and LS murine brains. These two transcripts have been shown to be generated by an alternative splicing event ocurring during the expression of the c-*jun* gene (22). The magnitude of the mAChR-mediated c-*jun* induction in both SS and LS mouse CNS was much lower, compared with the high level of induction (up to 9-fold increases over basal levels) of the c-*fos* gene. Oxotremorine-induced c-*jun* mRNA accumulations at 90 and 180 min were significantly larger in the LS mice than in the SS mice. Detectable increases of c-*jun* transcripts were observed at 30 and 60 min in SS and LS mice, respectively. Thus, the induction profile of c-*jun* in LS mice was different from that in SS mice, due to a delayed and more protracted expression of c-*jun* in LS mouse CNS (data not shown). The induced levels of c-*jun* mRNA in the brains of both mouse strains were found to be lower than the induced levels of c-*fos* mRNA in these mouse strains, as determined empirically from the intensities of hybridization signals corresponding to c-*jun* and c-*fos* mRNAs on autoradiograms obtained by Northern blotting after identical exposure times.

***jun*-B.** The *jun*-B gene was induced with c-*fos* and c-*jun* in the CNS of both SS and LS mice in response to oxotremorine. Maximum induction of *jun*-B was 3.5-fold higher than basal levels in the LS mice and 2.6-fold higher in the SS mice (Fig. 1B). Basal *jun*-B mRNA levels were barely detectable at time 0 in the CNS of both mouse strains. At the 45- and 60-min time points, oxotremorine-induced *jun*-B mRNA was significantly higher in LS mice, compared with SS mice. Interestingly, at 180 min *jun*-B induction was completely abolished (from a 3.5-fold increase at 60 min to 0.68-fold at 180 min) in LS mice, whereas the same response was attenuated by only 35% in SS mice (from a 2.6-fold increase at 90 min to 1.7-fold at 180 min) (Fig. 1B).

***jun*-D.** In contrast to the other two members of the *jun* family genes (c-*jun* and *jun*-B), oxotremorine failed to induce the expression of the *jun*-D gene in the CNS of either mouse strain (data not shown). No significant induction was seen from time 0 to 180 min after oxotremorine injection. Basal *jun*-D levels were found to be higher than the levels of any IEG used in this study and were approximately equal to β-actin mRNA levels in the murine CNS. This assessment was made empirically by comparing signal intensities corresponding to *jun*-D mRNA with those for other mRNA species studied under the same conditions during the course of RNA analysis via the Northern blotting procedure.

***Egr*-1.** Detectable increases in the *Egr*-1 mRNA levels were observed as early as 15 min after oxotremorine administration and peaked at 90 and 120 min for LS and SS mice, respectively (Fig. 1C). Basal *Egr*-1 mRNA levels were detectable at time 0, and maximum responses (expressed as increases over basal levels) were 2.8-fold and 3.9-fold for SS and LS mice, respectively (Fig. 1C). Although oxotremorine-induced *Egr*-1 responses seemed to be higher in the LS mice than in the SS mice at almost all time points (except the 15-min point), no significant differences were determined.

Dose-Response Results for Oxotremorine-Induced IEGs

To further characterize the pharmacological nature of the IEG inductions in response to oxotremorine, we used a wide range of increasing concentrations of oxotremorine (0, 0.05, 0.5, 1, 2, 3, 4, and 5 mg/kg) in both mouse strains. The oxotremorine doses used ranged from subtremorigenic doses of 0.05 mg/kg up to LD_{50} doses such as 5 mg/kg. The latter dose was found to be equivalent to an LD_{50} in the SS mice but not in the LS population. Saline-treated mice were used as controls. No increase in any IEG was found 60 min after mock injection. These results were verified via both Northern analysis and *in situ* hybridization experiments (see Figs. 3–6). Significant increases in c-*fos*, c-*jun*, *jun*-B, and *Egr*-1 mRNA levels were seen with doses between 0.5 and 1 mg/kg in both mouse strains, and the dose-response relationship resembled a typical pharmacological response as a result of a drug-receptor interaction (Fig. 2).

Effect of Scopolamine on Oxotremorine-Induced Expression of IEGs

Fig. 3 shows the effect of the well characterized mAChR antagonist scopolamine on the oxotremorine-induced accumulation of c-*fos*, c-*jun*, *jun*-B, and *Egr*-1 mRNAs in the SS and LS mouse CNS. Scopolamine (10 mg/kg) failed to induce any of these IEGs when given alone, whereas it was able to completely abolish the increase in the mRNAs of all these genes produced by oxotremorine (4 mg/kg), when oxotremorine was given 15 min after the administration of scopolamine, in both mouse strains.

CNS Distribution of IEG mRNAs

To further identify the regional pattern of mAChR-induced IEG expression in the SS and LS mouse CNS, we performed *in situ* hybridization using ^{33}P-labeled riboprobes complementary to specific portions of c-*fos*, c-*jun*, *jun*-B, and *Egr*-1 mRNAs. The basal expression of the c-*fos* gene in the CNS of the SS and LS mice was determined by quantitation of autoradiograms obtained from saline-treated mice. Very low basal c-*fos* mRNA levels were found in selected brain regions, such as the cerebral cortex, olfactory bulb, all fields of hippocampal formation, and cerebellum (Fig. 4, A and C). Striatal structures such as caudate nucleus and putamen were devoid of c-*fos* transcripts. Similarly, brainstem was not found to contain any c-*fos* mRNA. Oxotremorine injection resulted in a marked increase in the levels of c-*fos* transcripts in the brains of SS and LS mice, with very similar patterns of expression (Fig. 4, B and D; Table 1). The mAChR-induced c-*fos* mRNA accumulation was predominantly detected in thalamus > cerebellum ≥ frontal part of the cerebral cortex > olfactory bulb > occipital part of the cerebral cortex > hippocampus in the SS mice and thalamus ≫ olfactory bulb > frontal part of the cerebral cortex > cerebellum > occipital part of the cerebral cortex > hippocampus in the LS mice (Table 1). The quantitation of oxotremorine-induced c-*fos* mRNA levels in various CNS areas revealed greater inductions in almost all of the LS mouse CNS

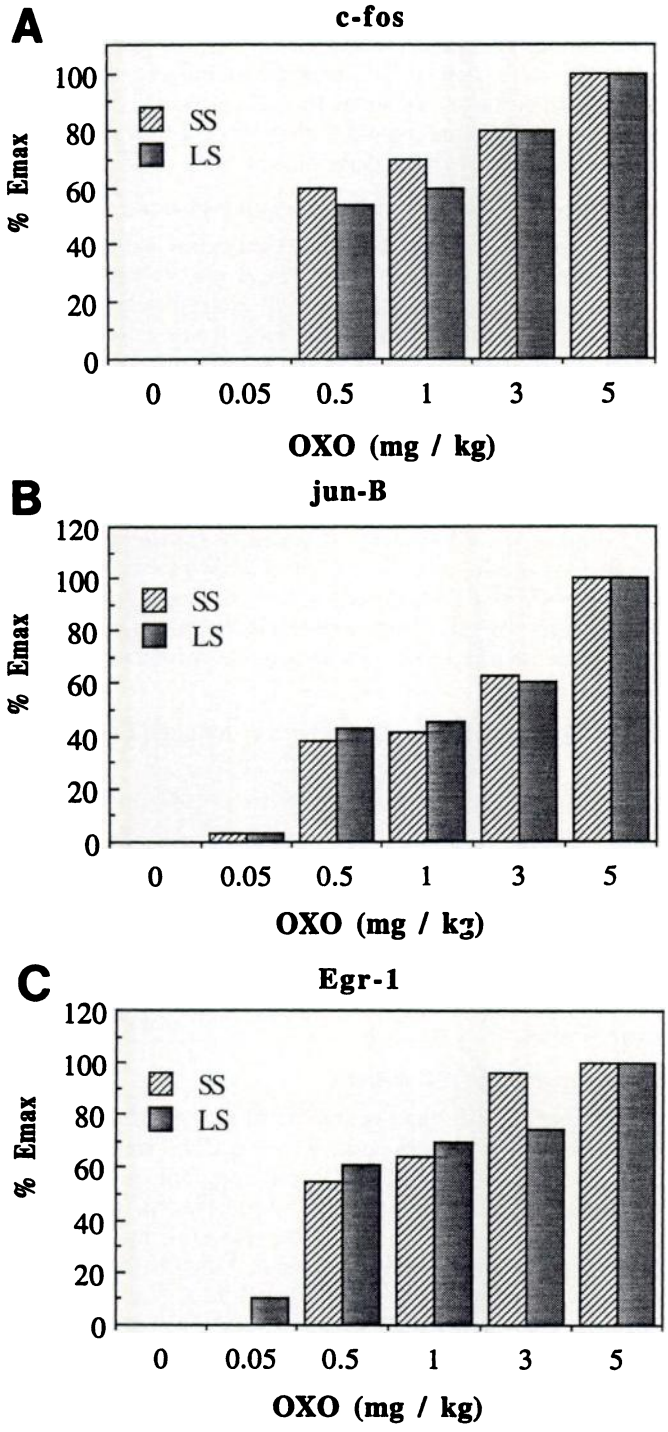

Fig. 2. Results of Northern RNA analyses showing the dose-response data for oxotremorine-induced c-*fos* (A), *jun*-B (B), and *Egr*-1 (C) expression in the CNS of SS and LS mice. Mice were given intraperitoneal injections of 0 (saline), 0.05, 0.5, 1, 2, 3, 4, or 5 mg/kg oxotremorine (*OXO*) and were sacrificed 60 min after the drug treatment. Alterations of each of c-*fos*, c-*jun*, *jun*-B, and *Egr*-1 mRNA levels were determined by Northern analysis and expressed as percentages of the net maximum responses (% *Emax*) obtained with 5 mg/kg oxotremorine in each mouse strain. These results were obtained from three to five separate experiments.

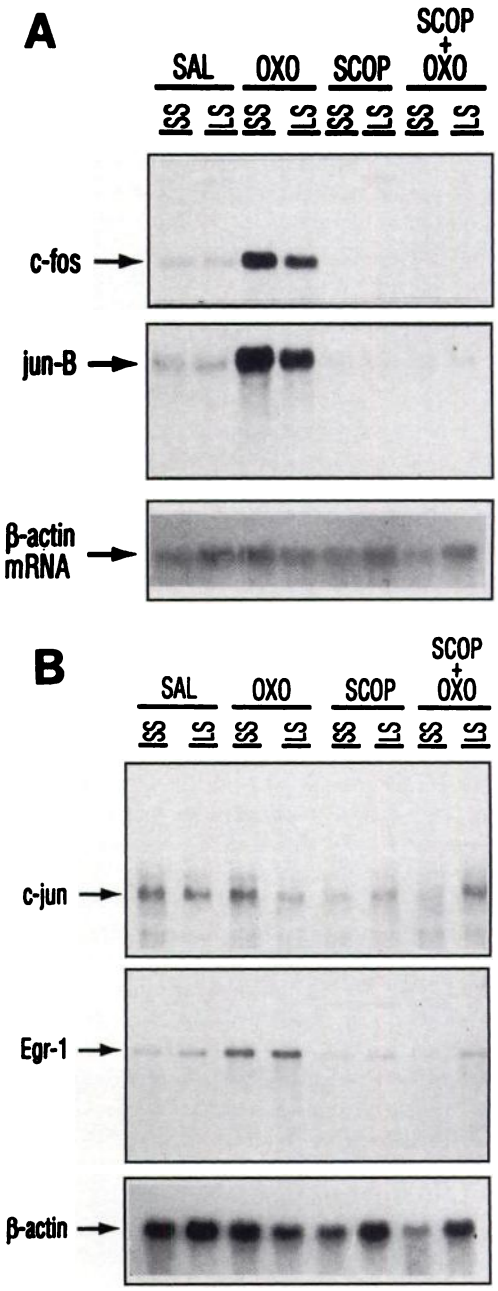

Fig. 3. Results of Northern RNA analyses showing the effect of scopolamine on oxotremorine-induced expression of c-*fos* and *jun*-B (A) and c-*jun* and *Egr*-1 (B) in the CNS of SS and LS mice. Mice were given intraperitoneal injections of saline (*SAL*), oxotremorine (*OXO*) (4 mg/kg), or scopolamine (*SCOP*) (10 mg/kg), or SCOP (10 mg/kg), 15 min before oxotremorine (4 mg/kg) and were sacrificed 60 min after the final treatment. Brains were excised and total RNA was purified as described in Materials and Methods. Ten micrograms of total RNA were loaded into each lane and electrophoresed through a 1.2% (w/v) agarose/6.6% (w/v) formaldehyde gel. Fractionated RNA was blotted onto nylon membranes and probed with c-*fos*, c-*jun*, *jun*-B, or *Egr*-1 ^{32}P-labeled antisense riboprobes (see Materials and Methods). Membranes were apposed to X-ray film with an intensifying screen for 3–4 days. The membranes were later probed with a β-actin ^{32}P-labeled antisense riboprobe to control for the quantity of the RNA loaded into each lane. Similar results were obtained from two independent experiments.

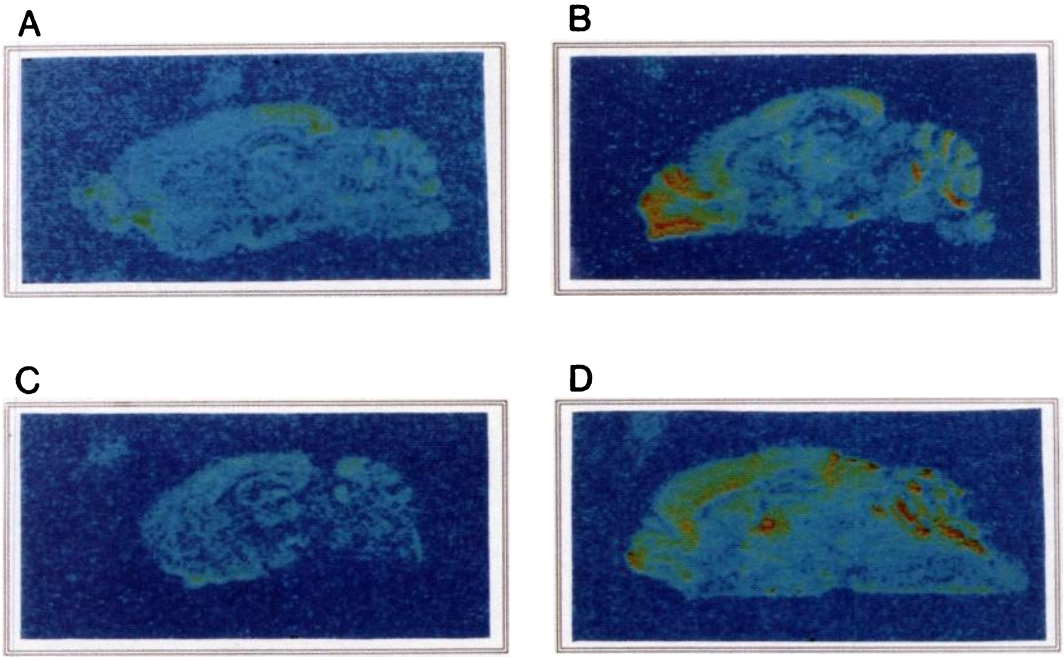

Fig. 4. Comparison of the CNS regional distribution of basal versus mAChR-induced c-*fos* expression in SS and LS mice. Results of *in situ* hybridization histochemistry show the distribution of c-*fos* transcripts in saline-treated SS mice (A), oxotremorine-treated (4 mg/kg, intraperitoneally) SS mice (B), saline-treated LS mice (C), and oxotremorine-treated LS mice (D). Serial sagittal sections (7-μm) obtained from mice sacrificed 60 min after drug or saline administration were hybridized with a ^{33}P-labeled c-*fos* antisense riboprobe derived from the *Eco*RI/*Sal*I fragment of c-*fos* cDNA and were apposed to Hyperfilm β-max film (Amersham) at −70° for 4 weeks. No signals were obtained using similarly labeled sense riboprobes assayed in parallel. See Materials and Methods for details.

TABLE 1

Regional distribution of c-*fos* transcripts in the CNS of saline- and oxotremorine-treated SS and LS mice

Results of *in situ* hybridization histochemistry, using film autoradiography are shown. SS and LS mice were given intraperitoneal injections of saline or 4 mg/kg oxotremorine and sacrificed 60 min after drug administration. Serial sagittal sections (7 μm) obtained from saline- and oxotremorine-treated SS and LS mouse brains were hybridized with a ^{33}P-labeled c-*fos* antisense riboprobe. See Methods and Materials for a detailed description. Values represent means ± standard errors from three to five separate determinations with two animals from each group, in two independent experiments. Statistical significance between saline- or oxotremorine-treated SS and LS mice was determined by one-way ANOVA with *post hoc* Newman-Keuls tests.

CNS region	Relative density				c-*fos* mRNA induction	
	Saline		Oxotremorine			
	SS	LS	SS	LS	SS	LS
	nCi/μg				*fold*	
Cerebral cortex						
Occipital	51 ± 7	28 ± 3	114 ± 5	194 ± 13[a]	2.2	6.9
Frontal	24 ± 4	15 ± 2	94 ± 4	152 ± 8[a]	3.9	10.0
Hippocampus	44 ± 7	25 ± 3	78 ± 8	107 ± 6[a]	1.7	4.3
Olfactory bulb	44 ± 7	12 ± 1	123 ± 12	132 ± 8	2.8	11.0
Thalamic structures	16 ± 3	7 ± 1	98 ± 9	156 ± 13[b]	6.0	22.0
Cerebellum	43 ± 7	21 ± 4	171 ± 16	188 ± 21	3.9	8.9

[a] $p < 0.01$.
[b] $p < 0.05$.

structures analyzed (Table 1) and further verified the results obtained by Northern blot analysis, which showed that oxotremorine produced overall 3.7- and 9-fold inductions of c-*fos* mRNA over basal levels in SS and LS mouse brains, respectively (Fig. 1A).

Basal c-*jun* mRNA expression was detected in hippocampus, cerebellum, thalamus, olfactory bulb, and cerebral cortex. The c-*jun* gene was predominantly expressed in the dentate gyrus of the hippocampus, which showed the greatest abundance of c-*jun* mRNA of all CNS regions analyzed. Oxotremorine produced a moderate (up to 2-fold) increase in the levels of c-*jun* mRNAs in various CNS areas of SS and LS mice, compared with the more dramatic induction seen with c-*fos* mRNA. Interestingly, no significant c-*jun* induction was seen in the dentate gyrus of either mouse strain. Similarly, oxotremorine failed to induce c-*jun* in the thalamus, the frontal part of the cerebral cortex, and the olfactory bulb in both mouse strains. The oxotremorine-mediated selective induction in the cerebellum, the CA1 region, and the occipital cerebral cortex in SS mice and in the cerebellum and the CA1 region but not the occipital cerebral cortex in LS mice may explain the overall higher level of induction of c-*jun* in SS mice, compared with LS mice, revealed by Northern blot RNA analysis (data not shown).

Oxotremorine produced an accumulation of *jun*-B mRNA in all CNS areas that were found to contain basal *jun*-B mRNA levels in LS mice (Fig. 5). The greatest induction (10-fold higher than basal levels) was seen in the CA1 field of hippocampus of LS mice, and the smallest induction (4-fold) was detected in the dentate gyrus of the same strain (Table 2). High levels of induction were also seen in cerebral cortex, caudate nucleus, and putamen of LS mice. In contrast, oxotremorine produced minimal inductions of *jun*-B in the cerebral cortex, CA1 field, and dentate gyrus of SS mice (Table 2).

The expression pattern of *jun*-B showed marked differences, compared with the distribution pattern of the other member of the *jun* family, c-*jun*. Cerebellum was found to express considerable basal c-*jun* mRNA levels and, moreover, oxotremorine was able to induce c-*jun* expression in cerebellum about 2-fold over basal levels in both mouse strains. However, the same region was devoid of basal *jun*-B expression and oxotremorine produced minimal induction of the *jun*-B gene in this area (Fig. 5). Another CNS structure showing differential expression of c-*jun* and *jun*-B was the hippocampus. Dentate gyrus was found to be the predominant region of basal c-*jun* expression in the hippocampus, in contrast to *jun*-B, which was found to be predominantly expressed in the CA1 field of the hippocampus. Moreover, *jun*-B was significantly induced in caudate nucleus and putamen, in contrast to c-*jun*, which was not induced by oxotremorine in these striatal structures (Fig. 5).

mAChR-induced expression of *Egr*-1 was detected predominantly in cerebral cortex, olfactory bulb, CA1 hippocampal field, and caudate nucleus and putamen in both mouse strains. The distribution patterns of both basal and oxotremorine-induced *Egr*-1 expression showed marked similarities to the corresponding patterns of *jun*-B, particularly in occipital cortex, CA1 field, and caudate nucleus and putamen (Figs. 5 and 6). Although Northern analysis failed to reveal any significant differences between SS and LS mice at 60 min, *in situ* hybridization experiments showed significantly greater inductions of *Egr*-1 mRNA in response to oxotremorine in all major CNS areas of the LS mice (Table 3).

CNS Distribution of m1–m5 mAChR mRNAs

We determined distributions and levels of all five mAChR subtype mRNAs by *in situ* hybridization using oligomers complementary to each of the five mAChR subtype mRNAs, to investigate whether these differences in the IEGs reflect regional differences in receptor numbers. No significant differences in the distributions and levels of m2–m5 mRNAs were found (data not shown). However, m1 mRNA levels were found to be 1.7-fold higher in the occipital cortex of the LS mice (Table 4). Although it is not certain whether increased m1 mRNA levels correspond to increased m1 receptor protein levels, membrane binding experiments using a somewhat M1-selective ligand, [^{3}H]pirenzipine, revealed no differences in the numbers of binding sites between LS and SS cerebral cortex (data not shown).

mAChR-Mediated Inositol Phosphate Hydrolysis

The responsiveness of the genotypes to mAChR agonist-induced inositol phosphate hydrolysis showed significant differences that are best observed with carbachol, which yielded the greatest response. Results showed that, whereas no significant differences in the K_{act} could be established between strains, due in part to the variable response data and the minimal response seen in SS mice, it is apparent that the E_{max}

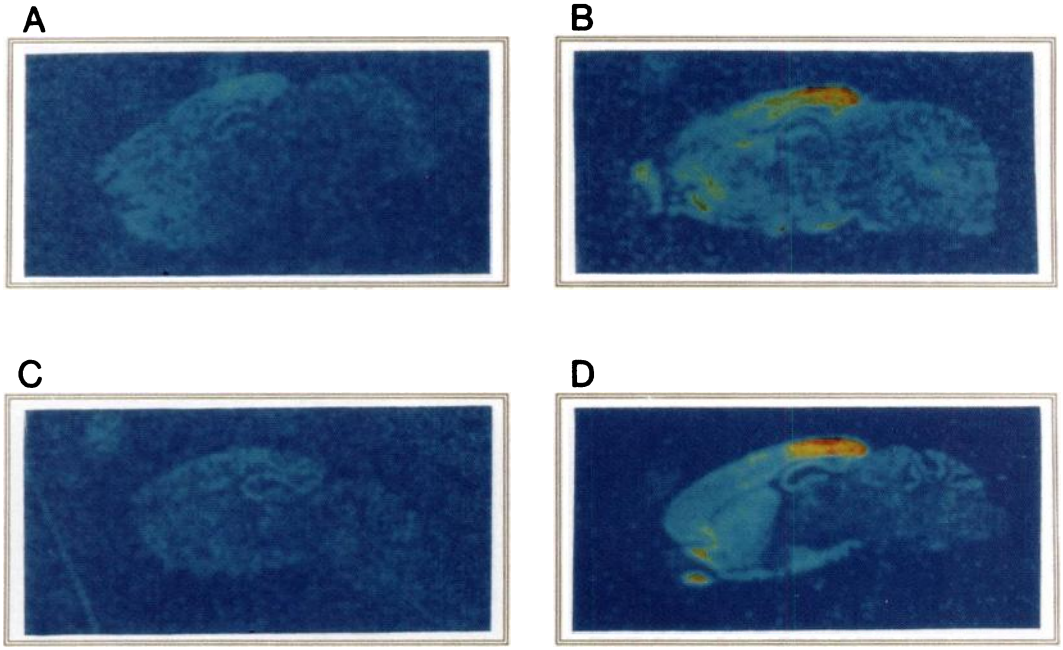

Fig. 5. Comparison of the CNS regional distribution of basal versus mAChR-induced *jun*-B expression in SS and LS mice. Results of *in situ* hybridization histochemistry show the distribution of *jun*-B transcripts in saline-treated SS mice (A), oxotremorine-treated (4 mg/kg, intraperitoneally) SS mice (B), saline-treated LS mice (C), and oxotremorine-treated LS mice (D). Serial sagittal sections (7 μm) obtained from mice sacrificed 60 min after drug or saline administration were hybridized with a ^{33}P-labeled *jun*-B antisense riboprobe derived from the *Bam*HI/*Bam*HI fragment of *jun*-B cDNA and were apposed to Hyperfilm β-max film (Amersham) at −70° for 4 weeks. No signals were obtained using similarly labeled sense riboprobes assayed in parallel. See Materials and Methods for details.

TABLE 2

Regional distribution of *jun*-B transcripts in the CNS of saline- and oxotremorine-treated SS and LS mice

Results of *in situ* hybridization histochemistry, using film autoradiography, are shown. SS and LS mice were given intraperitoneal injections of saline or 4 mg/kg oxotremorine and sacrificed 60 min after drug administration. Serial sagittal sections (7 μm) obtained from saline- and oxotremorine-treated SS and LS mouse brains were hybridized with a ^{33}P-labeled jun-B antisense riboprobe. See Materials and Methods for a detailed description. Values represent means ± standard errors from three to five separate determinations with two animals from each group, in two independent experiments. Statistical significance between saline- or oxotremorine-treated SS and LS mice was determined as described in Table 1.

CNS region	Relative density				*jun*-B mRNA induction	
	Saline		Oxotremorine			
	SS	LS	SS	LS	SS	LS
	nCi/μg				*fold*	
Cerebral cortex						
Occipital	63 ± 11	32 ± 2[a]	201 ± 33	262 ± 17[a]	3.2	8.0
Frontal	55 ± 10	17 ± 2	65 ± 9	153 ± 13[b]	1.1	9.0
Hippocampus						
CA1 field	77 ± 10	30 ± 8	121 ± 10	309 ± 25[b]	1.5	10.0
CA3 field	34 ± 9	30 ± 12	82 ± 14	147 ± 10[b]	2.4	5.0
Dentate gyrus	64 ± 6	34 ± 8	101 ± 21	139 ± 10[a]	1.6	4.0
Olfactory bulb	71 ± 5	27 ± 4[a]	144 ± 2	224 ± 15[b]	2.0	8.3
Caudate nucleus and putamen	37 ± 5	20 ± 1	87 ± 12	160 ± 10[b]	2.3	8.0

[a] $p < 0.05$.
[b] $p < 0.01$

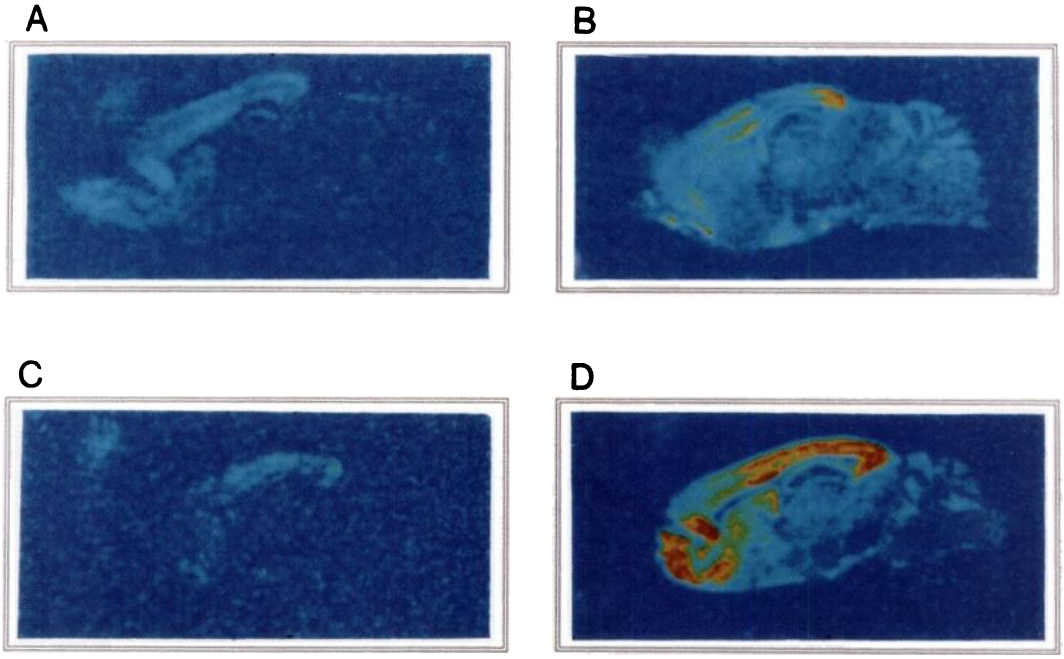

Fig. 6. Comparison of the CNS regional distribution of basal versus mAChR-induced *Egr*-1 expression in SS and LS mice. Results of *in situ* hybridization histochemistry show the distribution of *Egr*-1 transcripts in saline-treated SS mice (A), oxotremorine-treated (4 mg/kg, intraperitoneally) SS mice (B), saline-treated LS mice (C), and oxotremorine-treated LS mice (D). Serial sagittal sections (7 μm) obtained from mice sacrificed 60 min after drug or saline administration were hybridized with a ^{33}P-labeled *Egr*-1 antisense riboprobe derived from the *BglII/RsaI* fragment of *Egr*-1 cDNA and were apposed to Hyperfilm β-max film (Amersham) at −70° for 4 weeks. No signals were obtained using similarly labeled sense riboprobes assayed in parallel. See Materials and Methods for details.

values differ considerably. Both LS and SS mice yielded K_{act} values equal to 1×10^{-4} M, but the LS mice showed a 5-fold higher E_{max} value than did SS mice in a comparison of parallel concentration-effect curves for the atropine-reversible accumulation of [^{3}H]inositol-1-phosphate induced by carbachol administration in the cerebral cortex.

Discussion

Studies show that mAChR activation induces several IEGs, such as c-*fos*, *fos*-B, *fra*-2, c-*jun*, *jun*-B, *jun*-D, *Egr*-1 (*NGFI-A/krox24/zif268/TIS-8/d-2*), *TIS-1* (*NGFI-B/nur77*), *TIS-7* (*PC4*), *TIS-11*, and c-*myc*, in various cell culture systems (23–28). Previous data also showed that mAChR activation by pilocarpine induces increased c-*fos* mRNA levels in the cerebral cortex and hippocampus (29), Fos/Fra levels in the rat CNS (30), and *jun*-B mRNA and protein levels in rat hippocampal and striatal neurons (31). Our studies show that intraperitoneal oxotremorine administration produces a dose-dependent, region-specific, coordinated induction of c-*fos*, c-*jun*, *jun*-B, and *Egr*-1 but not *jun*-D mRNA in the murine brain. These inductions were inhibited by mAChR antagonist administration, demonstrating an involvement of mAChR systems in initiating these genomic responses.

A precise role for mAChR system contributions to these IEG inductions remains to be defined, due to downstream events

TABLE 3

Regional distribution of *Egr*-1 transcripts in the CNS of saline- and oxotremorine-treated SS and LS mice

Results of *in situ* hybridization histochemistry, using film autoradiography, are shown. SS and LS mice were given intraperitoneal injections of saline or 4 mg/kg oxotremorine and sacrificed 60 min after drug administration. Serial sagittal sections (7 μm) obtained from saline- and oxotremorine-treated SS and LS mouse brains were hybridized with a ^{33}P-labeled *Egr*-1 antisense riboprobe. See Materials and Methods for a detailed description. Values represent means ± standard errors from three to five separate determinations with two animals from each group, in two independent experiments. Statistical significance between saline- or oxotremorine-treated SS and LS mice was determined as described in Table 1.

CNS region	Relative density				*Egr*-1 mRNA induction	
	Saline		Oxotremorine			
	SS	LS	SS	LS	SS	LS
	nCi/μg				*fold*	
Cerebral cortex						
Occipital	28 ± 8	25 ± 7	196 ± 24	292 ± 29[a]	7.0	12.0
Frontal	39 ± 5	23 ± 1	157 ± 23	275 ± 24[a]	4.0	12.0
Hippocampus						
CA1 field	41 ± 5	20 ± 3	152 ± 18	185 ± 26	3.7	9.0
CA3 field	20 ± 4	20 ± 3	66 ± 8	114 ± 20[a]	3.3	5.7
Dentate gyrus	29 ± 12	12 ± 1	68 ± 9	104 ± 14[a]	2.3	8.6
Caudate nucleus and putamen	21 ± 2	18 ± 3	92 ± 14	137 ± 18[b]	4.4	11.4

[a] $p < 0.01$.
[b] $p < 0.05$.

TABLE 4

Regional distribution of m1 mAChR subtype mRNA in SS and LS mice

Results of quantitative *in situ* hybridization histochemistry, using film autoradiography, are shown. See Materials and Methods for details. Values represent means ± standard errors from three to nine separate determinations in three or more independent experiments. Statistical significance was determined with one-way ANOVA and *post hoc* Newman-Keuls tests.

CNS region	Relative density	
	SS	LS
	nCi/μg	
Cerebral cortex		
Occipital	73 ± 9	125 ± 16[a]
Frontal	95 ± 10	113 ± 14
Hippocampus		
CA1 field	132 ± 20	136 ± 20
CA3 field	84 ± 9	133 ± 19
Dentate gyrus	208 ± 30	211 ± 30
Olfactory bulb	448 ± 20	405 ± 30
Piriform cortex	224 ± 50	206 ± 50
Caudate nucleus and putamen	80 ± 30	86 ± 15

[a] $p < 0.05$.

that may induce various IEGs. These downstream events include complex transsynaptic interactions involving other neurotransmitter systems or "nonsynaptic" events such as tremors, regional hypoxia, or hypotension. Agents such as pentylenetetrazole and metrazole, which produce increased CNS electical activity and act on different neurotransmitter systems, do not show the same IEG induction profiles after oxotremorine administration. Specifically, pentylenetetrazole or metrazole administration results in a significant induction of c-*jun* and *fra*-1 in the hippocampus (32, 33), in contrast to oxotremorine, pilocarpine, and carbachol, which are not able to induce these genes *in vivo* (31) or in cell culture (23). Moreover, bicuculline was found to induce Jun-D protein in the rat hippocampus (34), whereas our studies failed to show any oxotremorine-induced expression of *jun*-D in any brain region analyzed. In support of the concept that mAChR activation results in a unique IEG profile, studies on the hypoxia-inducible IEGs have shown a robust induction of *jun*-D, along with other members of the *jun* and *fos* families (35–37). In contrast to these results, we never observed any *jun*-D induction by oxotremorine. Other possible downstream events, such as hypotension or stress, have been found to preferentially induce c-*fos* in supraoptic vasopressin neurons (38) and in other brainstem structures (39). Our results revealed a markedly distinct distribution of c-*fos* mRNA in oxotremorine-treated mice and thus differentiate IEG expression from hypoxia, hypotension, stress, and other, more generalized, IEG inductions.

Because SS and LS mice show differential responsiveness and sensitivity to mAChR agonist or antagonist treatment, we investigated whether oxotremorine, a mAChR agonist, differentially induces c-*fos* mRNA levels in SS versus LS mouse CNS. Indeed, greater induction of c-*fos*, *jun*-B, and *Egr*-1 mRNA were seen in LS mice after drug administration, as shown by both Northern and *in situ* hybridization analyses. Because these differential IEG inductions might be attributed to regional differences in receptor numbers that could further complicate the interpretation of our results using oxotremorine, which is a partial agonist, we also determined m1–m5 mAChR mRNA levels in the CNS of both strains. Only minor differences were seen, with the difference in m1 mRNA levels being the only significant difference observed. It is questionable whether this alone may account for the overall higher IEG inductions in the LS mice, particularly because this was seen only in the occipital cortex. Rather, different coupling constraints in the two strains may be a crucial factor.

Several lines of evidence suggest an m2-mediated c-*fos* induction by oxotremorine. First, a regional correlation between oxotremorine-induced c-*fos* mRNA and m2 mAChRs is evident. Specifically, the predominant mAChR subtype in thalamus and cerebellum is m2, whereas in hippocampus m2 is barely detectable (18, 40–43). Similarly, the greatest induction of c-*fos* was seen in thalamus and cerebellum, whereas the smallest was in the hippocampus. Second, oxotremorine likely has somewhat greater efficacy for m2/m4 than for m1/m3 or m5 mAChRs (44). Third, *in vitro* studies support the concept of m2-mediated c-*fos* induction. Activation of m2 receptors by carbachol was able to induce c-*fos* mRNA in Chinese hamster ovary cells stably transfected with the m2 subtype gene. Although carbachol-induced c-*fos* mRNA was more robust in m1-transfected cells, compared with m2-transfected cells, only m2-mediated c-*fos* induction was completely inhibited by PTX, suggesting the involvement of PTX-sensitive G proteins in m2-mediated c-*fos*

induction (26). Dell'Acqua *et al.* (45) also identified the G_i species associated with the m2 receptor in these cells, including $G_{\alpha i2}$ and $G_{\alpha i3}$. However, it is not clear whether $G_{\alpha i2}$ and/or $G_{\alpha i3}$ are involved in a signaling pathway that is triggered by m2 receptor activation and ends with the induction of c-*fos*. It has been proposed that thrombin, whose signaling pathway shares some common characteristics with the signaling pathway triggered by mAChR activation, exerts its PTX-sensitive mitogenic effects on CCL39 hamster fibroblasts via activation of $G_{\alpha i2}$ and $G_{\alpha i3}$, phosphorylation of a number of proteins such as mitogen-activated protein kinase and c-*raf*, and induction of several IEGs such as c-*fos* and c-*jun* (27, 46). Interestingly, a recent report showed that m2, but not m1, receptor stimulation results in the activation of the Ras/Raf/mitogen-activated protein kinase pathway via G_i proteins in Rat-1a cells stably transfected with m1 or m2 receptor genes (47). Taken together, these findings indicate that differential expression of regulatory proteins such as $G_{\alpha i2}$ and/or $G_{\alpha i3}$ may result in differential induction of c-*fos*, whose expression is likely regulated via CNS m2 receptors in these mice. Notably, the involvement of G proteins in mediating the effects of ethanol has been recently reviewed elsewhere (48). Also, it was shown that chronic ethanol treatment of NG108–15 and NCB-20 cells produces marked reductions in $G_{\alpha i2}$ (49). Genetic alterations in the expression of $G_{\alpha i2}$ in SS mouse CNS areas rich in m2 receptors may prove to be a crucial factor underlying differential c-*fos* induction among these two murine strains.

mAChR-mediated induction of c-*jun* in cell culture, and specifically by pilocarpine in the hippocampus, has been somewhat ambiguous (23, 31). Our Northern and *in situ* experiments showed that maximum inductions were 2-fold in selected CNS regions in both strains. Notably, the lowest induced levels were observed in the dentate gyrus, which also showed the highest basal expression levels. There is no apparent reason for the failure of oxotremorine to produce a significant induction of c-*jun* in the dentate gyrus, but one may be tempted to speculate that essential second messenger systems coupled to mAChR subtypes in the dentate gyrus, whose stimulation is required for c-*jun* induction, may not be efficiently activated by oxotremorine under our *in vivo* experimental circumstances. Similarly, Dragunow *et al.* (31) recently showed extremely weak hippocampal c-*jun* induction with pilocarpine.

Similarly to the greater induction of c-*fos* mRNA in LS mice, *jun*-B and *Egr*-1 inductions were also greater in the same strain. These differences were noted in almost every brain region analyzed and suggest a differential coupling of mAChR activation and *jun*-B and *Egr*-1 induction. In addition to the differential induction of *jun*-B and *Egr*-1 at the 60-min time point, induction levels of *jun*-B mRNA were significantly higher in SS, compared with LS, mouse CNS at 180 min. Because we do not have adequate data to conclusively address this, it is uncertain whether Jun-B protein follows the same kinetic pattern as the mRNA. However, it is logical to speculate that mAChR activation results in significantly greater levels of Jun-B protein in SS versus LS mouse CNS at later time points. This protein may exert specific functional effects on the transcription of downstream genes. The striking similarities of the induction patterns of *jun*-B and *Egr*-1 mRNAs in response to oxotremorine suggest that oxotremorine produces these responses via very similar signaling pathways that seem to be distinct from those that mediate the induction of c-*fos* or c-*jun*. These findings cause us to speculate that the relative abundance of each mAChR subtype and its corresponding second messenger systems in specific brain areas predominantly determines the nuclear response.

In contrast to c-*fos*, c-*jun*, *jun*-B, and *Egr*-1, *jun*-D was not induced by oxotremorine in either strain. However, high levels of *jun*-D mRNA were noted in both Northern and *in situ* hybridization experiments. Its constitutively high levels of expression and its widespread distribution suggest a critical role of this gene in the modulation of basal transcription of AP-1-responsive genes in the murine CNS. The physiological significance of *jun*-D may be in regulating basal expression of crucial genes for "normal" ongoing CNS function.

Although the precise physiological role of IEG induction by oxotremorine is not known, these genes may produce long term changes in cellular phenotypes, such as neuronal plasticity and adaptation, or cell growth and mitogenesis. Because the *in vivo* mAChR-induced c-*fos*, c-*jun*, *jun*-B, and *Egr*-1 mRNA increases occurred in postmitotic neurons of the adult CNS, they are likely associated with functions other than cell proliferation in the CNS. Indeed, it has been shown that carbachol activates the transcription of c-*fos* only in neuronal cells and not in glial cells (50), and oxotremorine is not able to induce proliferation of astrocytes in primary cultures (51). These findings, taken together with our data, strongly suggest that mAChR-mediated IEG induction serves other functions besides astrocytic proliferation in the adult CNS. One likely process may be neuronal adaptation to the consequences of initial receptor activation. Thus, our demonstration of differential induction of these proto-oncogenes in the CNS of SS versus LS mice provides a molecular basis for the differential behavioral responsiveness of these two strains to ethanol as well as to mAChR-specific agents.

Acknowledgments

We thank S. Vincent, J. J. McArdle, and S. Christakos for helpful discussions and F. Ehlert for valuable comments and criticisms on the manuscript. We also thank L. Cho for back-up use of a cryostat.

References

1. Deitrich, R. A., T. V. Dunwiddie, R. A. Haris, and V. G. Erwin. Mechanism of action of ethanol: initial central nervous system actions. *Pharmacol. Rev.* **41**:489–537 (1989).
2. Erickson, C. K., and D. T. Graham. Alteration of cortical and reticular acetylcholine release by ethanol *in vivo*. *J. Pharmacol. Exp. Ther.* **185**:583–593 (1973).
3. Carmichael, F. J., and Y. Israel. Effects of ethanol on neurotransmitter release by rat brain cortical slices. *J. Pharmacol. Exp. Ther.* **193**:824–834 (1975).
4. Phillis, J. W., Z. G. Jiang, and B. J. Chelack. Effect of ethanol on acetylcholine and adenosine efflux from the *in vivo* rat cerebral cortex. *J. Pharm. Pharmacol.* **32**:871–872 (1980).
5. Tabakoff, B., M. Munoz-Marcus, and J. Z. Fields. Chronic ethanol feeding produces an increase in muscarinic cholinergic receptors in mouse brain. *Life Sci.* **25**:2173–2180 (1979).
6. Rabin, R. A., B. B. Wolfe, M. D. Dibner, M. R. Zahniser, C. Melchior, and P. B. Molinoff. Effects of ethanol administration and withdrawal on neurotransmitter receptor systems in C57 mice. *J. Pharmacol. Exp. Ther.* **213**:491–496 (1980).
7. Smith, T. L. Influence of chronic ethanol consumption on muscarinic cholinergic receptors and their linkage to phospholipid metabolism in mouse synaptosomes. *Neuropharmacology* **22**:661–663 (1983).
8. McClearn, G. E., and R. Kakihana. Selective breeding for ethanol sensitivity in mice. *Behav. Genet.* **3**:409–410 (1973).
9. Watson, M., L. Tsiokas, S. Vincent, X. Ming, S. C. Zhang, and J. J. McArdle. *In situ* hybridization, inositol phospholipid hydrolysis and receptor localization studies of CNS muscarine receptor subtypes show differential distributions in long-sleep and short-sleep mice. *Eur. J. Pharmacol.* **183**:1620 (1990).
10. McArdle, J. J., S. P. Aiken, G. Huang, L. Tsiokas, X. Ming, S. Vincent, S. C. Zhang, and M. Watson. Insights into the molecular mechanism of action of ethanol on brain calcium channels and muscarinic acetylcholine receptors derived from long and short sleep mice, in *Alcohol and Neurobiology: Recep-*

tors, Membranes, and Channels (R. Watson, ed.). CRC Press, Boca Raton, FL, 127–139 (1992).
11. Erwin, V. G., A. Korte, and B. C. Jones. Central muscarinic cholinergic influences on ethanol sensitivity in long-sleep and short-sleep mice. *J. Pharmacol. Exp. Ther.* **247**:857–862 (1988).
12. Rauscher, F. J., III, P. J. Voulalas, R. Franza, Jr., and T. Curran. Fos and Jun bind cooperatively to the AP-1 site: recognition *in vitro*. *Genes Dev.* **2**:1687–1699 (1989).
13. Sukhatme, V. P., X. Cao, L. C. Chang, C.-H. Tsai-Morris, D. Stamenkovich, P. C. P. Ferreira, D. R. Cohen, S. A. Edwards, T. B. Shows, T. Curran, M. M. Le Beau, and E. D. Adamson. A zinc finger-encoding gene coregulated with c-*fos* during growth and differentiation, and after cellular depolarization. *Cell* **53**:37–43 (1988).
14. Hirai, S. I., R.-P. Ryseck, F. Mechta, R. Bravo, and M. Yaniv. Characterization of *jun*-D: a new member of the *jun* proto-oncogene family. *EMBO J.* **8**:1433–1439 (1989).
15. Cox, K. H., D. V. DeLeon, L. M. Angerer, and R. C. Angerer. Detection of mRNAs in sea urchin embryos by *in situ* hybridization using asymmetric RNA probes. *Dev. Biol.* **101**:485–502 (1984).
16. Chomczynski, P., and N. Sacchi. Single-step method of RNA isolation by acid guanidinium thiocyanate-phenol-chloroform extraction. *Anal. Biochem.* **162**:156–159 (1987).
17. Baldino, F., Jr., M.-F. Chesselet, and M. E. Lewis. High resolution *in situ* hybridization histochemistry, in *Neuroendocrine Peptide Methodology* (P. M. Conn, ed.). Academic Press, New York, 79–95 (1989).
18. Buckley, N. J., T. I. Bonner, and M. R. Brann. Localization of a family of muscarinic receptor mRNAs in rat brain. *J. Neurosci.* **8**:4646–4652 (1988).
19. Weiner, D. M., A. I. Levey, and M. R. Brann. Expression of muscarinic acetylcholine and dopamine receptor mRNAs in rat basal ganglia. *Proc. Natl. Acad. Sci. USA* **87**:7050–7054 (1990).
20. Bonner, T. I., N. J. Buckley, A. C. Young, and M. R. Brann. Identification of a family of muscarinic acetylcholine receptor genes. *Science (Washington D. C.)* **237**:527–532 (1987).
21. Lewis, M. E., W. T. Rogers, R. G. Krause II, and J. S. Schwaber. Quantitation and digital representation of hybridization histochemistry. *Methods Enzymol.* **168**:808–821 (1989).
22. Ryseck, R.-P., S. I. Hirai, M. Yaniv, and R. Bravo. Transcriptional activation of c-*jun* during the G_o/G_i transition in mouse fibroblasts. *Nature (Lond.)* **334**:535–537 (1989).
23. Trejo, J., J.-C. Chambard, M. Karin, and J. H. Brown. Biphasic increase in c-*jun* mRNA is required for induction of AP-1-mediated gene transcription: differential effects of muscarinic and thrombin receptor activation. *Mol. Cell. Biol.* **12**:4742–4750 (1992).
24. Blackshear, P. J., D. J. Stumpo, J.-K. Huang, R. A. Nemenoff, and D. H. Spach. Protein kinase C-dependent and -independent pathways of proto-oncogene induction in human astrocytoma cells. *J. Biol. Chem.* **262**:7774–7781 (1987).
25. Trejo, J., and J. H. Brown. c-*fos* and c-*jun* are induced by muscarinic receptor activation of protein kinase C but are differentially regulated by intracellular calcium. *J. Biol. Chem.* **266**:7876–7882 (1991).
26. Ashkenazi, A., E. G. Peralta, J. W. Winslow, J. Ramachandran, and D. J. Capon. Functional diversity of muscarinic receptor subtypes in cellular signal transduction and growth. *Trends Pharmacol. Sci.* **10**(suppl.):16–22 (1989).
27. Seuwen, K., C. Kahan, T. Hartmann, and J. Pouyssegur. Strong and persistent activation of inositol lipid breakdown induces early mitogenic events but not G_0 to S phase progression in hamster fibroblasts. *J. Biol. Chem.* **265**:22292–22299 (1990).
28. Arenander, A. T., J. de Vellis, and H. R. Herschman. Induction of c-*fos* and *TIS* genes in cultured rat astrocytes by neurotransmitters. *J. Neurosci. Res.* **24**:107–114 (1989).
29. Weiner, E. D., V. D. Kalasapudi, D. F. Papolos, and H. M. Lachman. Lithium augments pilocarpine-induced *fos* gene expression in rat brain. *Brain Res.* **553**:117–122 (1991).
30. Hughes, P., and M. Dragunow. Muscarinic receptor-mediated induction of Fos protein in rat brain. *Neurosci. Lett.* **150**:122–126 (1993).
31. Dragunow, M., D. Young, P. Hughes, G. MacGibbon, P. Lawlor, K. Singleton, E. Sirimanne, E. Beilharz, and P. Gluckman. Is c-*jun* involved in nerve cell death following status epilepticus and hypoxic-ischaemic brain injury? *Mol. Brain Res.* **18**:347–352 (1993).
32. Sonnenberg, J. L., P. F. Macgregor-Leon, T. Curran, and J. I. Morgan. Dynamic alterations occur in the levels and composition of transcription factor AP-1 complexes after seizure. *Neuron* **3**:359–365 (1989).
33. Sonnenberg, J. L., F. J. Rauscher III, J. I. Morgan, and T. Curran. Regulation of proenkephalin by Fos and Jun. *Science (Washington D. C.)* **246**:1622–1625 (1989).
34. Gass, P., T. Herdegen, R. Bravo, and M. Kiessling. Induction of immediate early gene encoded proteins in the rat hippocampus after bicuculline-induced seizures: differential expression of Krox-24, Fos and Jun proteins. *Neuroscience* **48**:315–324 (1992).
35. Webster, K. A., D. J. Discher, and N. H. Bishopric. Induction and nuclear accumulation of *fos* and *jun* proto-oncogenes in hypoxic cardiac myocytes. *J. Biol. Chem.* **268**:16852–16858 (1993).
36. Goldberg, M. A., and T. J. Schneider. Similarities between the oxygen-sensing mechanisms regulating the expression of vascular endothelial growth factor and erythropoietin. *J. Biol. Chem.* **269**:4355–4359 (1994).
37. Ausserer, W. A., B. Bourrat-Floeck, C. J. Green, K. R. Laderoute, and R. M. Sutherland. Regulation of c-*jun* expression during hypoxic and low-glucose stress. *Mol. Cell. Biol.* **14**:5032–5042 (1994).
38. Shen, E., S. L. Dun, C. Ren, C. Bennett-Clarke, and N. J. Dun. Hypotension preferentially induces c-*fos* immunoreactivity in supraoptic vasopressin neurons. *Brain Res.* **593**:136–139 (1992).
39. Naranjo, J. R., B. Mellstrom, M. Achaval, J. J. Lucas, J. Del Rio, and P. Sassone-Corsi. Co-induction of *jun*-B and c-*fos* in a subset of neurons in the spinal cord. *Oncogene* **6**:223–227 (1991).
40. Li, M., R. P. Yasuda, S. J. Wall, A. Wellstein, and B. B. Wolfe. Distribution of m2 muscarinic receptors in rat brain using antisera selective for m2 receptors. *Mol. Pharmacol.* **40**:28–35 (1991).
41. Levey, A. I., C. A. Kitt, W. F. Simonds, D. L. Price, and M. R. Brann. Identification of muscarinic acetylcholine receptor proteins in brain with subtype-specific antibodies. *J. Neurosci.* **11**:3218–3226 (1991).
42. Cortes, R., and J. M. Palacios. Muscarinic cholinergic receptor subtypes in the rat brain. 1. Quantitative autoradiographic studies. *Brain Res.* **362**:227–238 (1986).
43. Mash, D. C., and L. T. Potter. Autoradiographic localization of M1 and M2 muscarine receptors in the rat brain. *Neuroscience* **19**:551–564 (1986).
44. Gil, D. W., and B. B. Wolfe. Pirenzipine distinguishes between muscarinic receptor-mediated phosphoinositide breakdown and inhibition of adenylate cyclase. *J. Pharmacol. Exp. Ther.* **232**:608–616 (1985).
45. Dell'Acqua, M. L., R. C. Carroll, and E. G. Peralta. Transfected m2 muscarinic acetylcholine receptors couple to G_{ai2} and G_{ai3} in Chinese hamster ovary cells. *J. Biol. Chem.* **268**:5676–5685 (1993).
46. Kahan, C., K. Seuwen, S. Meloche, and J. Pouyssegur. Coordinated, biphasic activation of p44 mitogen-activated protein kinase and S6 kinase by growth factors in hamster fibroblasts: evidence for thrombin-induced signals different from phosphoinositide turnover and adenylyl cyclase inhibition. *J. Biol. Chem.* **267**:13369–13375 (1992).
47. Russell, M., S. Winitz, and G. L. Johnson. Acetylcholine muscarinic m1 receptor regulation of cyclic AMP synthesis controls growth factor stimulation of Raf activity. *Mol. Cell. Biol.* **14**:2343–2351 (1994).
48. Hoffman, P. L., and B. Tabakoff. Ethanol and guanine nucleotide binding proteins: a selective interaction. *FASEB J.* **4**:2612–2622 (1990).
49. Williams, R. J., M. A. Veale, P. Horne, and E. Kelly. Ethanol differentially regulates guanine nucleotide-binding protein α subunit in NG108–15 cells independently of extracellular adenosine. *Mol. Pharmacol.* **43**:158–166 (1993).
50. Smeyne, R. J., K. Schilling, L. Robertson, D. Luk, J. Oberdick, T. Curran, and J. I. Morgan. *Fos-lacZ* transgenic mice: mapping sites of gene induction in the central nervous system. *Neuron* **8**:13–23 (1992).
51. Ashkenazi, A., J. Ramachandran, and D. J. Capon. Acetylcholine analogue stimulates DNA synthesis in brain-derived cells via specific muscarinic receptor subtypes. *Nature (Lond.)* **340**:146–150 (1989).

Send reprint requests to: Leonidas Tsiokas, Department of Medicine, Renal Division DA 517, Beth Israel Hospital, Harvard Medical School, 330 Brookline Ave., Boston, MA 02215.